Assessing Wear Coefficient and Predicting Surface Wear of Polymer Gears: A Practical Approach

Enis Muratovic
Faculty of Mechanical Engineering, University of Sarajevo, Sarajevo, Bosnia and Herzegovina
muratovic@mef.unsa.ba

Adil Muminovic
Faculty of Mechanical Engineering, University of Sarajevo, Sarajevo, Bosnia and Herzegovina
muminovic@mef.unsa.ba

Nedim Pervan
Faculty of Mechanical Engineering, University of Sarajevo, Sarajevo, Bosnia and Herzegovina
pervan@mef.unsa.ba (corresponding author)

Muamer Delic
Faculty of Mechanical Engineering, University of Sarajevo, Sarajevo, Bosnia and Herzegovina
delic@mef.unsa.ba

Adis Muminovic
Faculty of Mechanical Engineering, University of Sarajevo, Sarajevo, Bosnia and Herzegovina
adis.muminovic@mef.unsa.ba

Isad Saric
Faculty of Mechanical Engineering, University of Sarajevo, Sarajevo, Bosnia and Herzegovina
saric@mef.unsa.ba

Received: 5 April 2024 | Revised: 30 April 2024 and 9 May 2024 | Accepted: 18 May 2024

 DOI: https://doi.org/10.48084/etasr.7421

ABSTRACT

With the ever-increasing number of polymer materials and the current number of commercially available materials, the polymer gear design process, regarding the wear lifetime predictions, is a difficult task given that there are very limited data on wear coefficients that can be deployed to evaluate the wear behavior of polymer gears. This study focuses on the classic steel/polymer engagements that result in a wear-induced failure of polymer gears and proposes a simple methodology based on the employment of optical methods that can be used to assess the necessary wear coefficient. Polymer gear testing, performed on an open-loop test rig, along with VDI 2736 guidelines for polymer gear design, serves as a starting point for the detailed analysis of the wear process putting into service a digital microscope that leads to the evaluation of the wear coefficient. The same wear coefficient, as presented within the scope of this study, can be implemented in a rather simple wear prediction model, based on Archard's wear formulation. The developed model is established on the iterative numerical procedure that accounts for the changes in tooth flank geometry due to wear and investigates the surface wear impact on the contact pressure distribution to completely describe the behavior of polymer gears in different stages of their lifetime. Although a simple one, the developed wear prediction model is sufficient for most engineering applications, as the model prediction and experimental data agree well with each other, and can be utilized to reduce the need to perform time-consuming testing.

Keywords-polymer gear; wear coefficient; experimental testing; wear prediction model

I. INTRODUCTION

Recent trends in engineering practice are directed toward the application of lightweight components as a substitute for classic metal components [1]. When it comes to power transmission systems conventional metal gears are often replaced with polymer gears due to the numerous advantages the latter offer, such as smaller mass, easier and versatile manufacturing, better vibration damping, satisfactory noise properties, the potential to work in dry friction conditions, etc. However, polymer gear utilization is still quite limited since many unknown operational parameters restrict the possibility of predicting the gear behavior in real-life applications, like critical working conditions. Such parameters, involving thermal overload and excessive wear, which occur due to polymer material properties, need to be avoided [2-3]. The design process of polymer gears is even more difficult with the ever-increasing number of polymer materials, which require extensive experimental testing for the relevant gear design parameter to be ontained [4, 5]. Standard polymer gear engagement implies steel/polymer meshing without lubrication, where steel pinion's countersurface, due to higher thermal conductivity, neglects most of the temperature effects on the polymer gear [6, 7]. Although this standard configuration seems to have many benefits in terms of temperature-dependant polymer material properties, the hardness dissimilarity between meshing surfaces leads to the wear of the polymer gear tooth flank, which results in a tooth profile error in comparison with the theoretical involute geometry [8, 9]. During the engagement of steel pinion and polymer gear, micro-asperities of the steel surface penetrate through the softer polymer material causing an abrasive wear mechanism. The loss of material owing to surface wear causes constant changes in contact topography, where, apart from the direct material loss that leads to failure, gear engagement patterns are changed in a way that contact pressure distribution is altered to accelerate the other failure mechanisms [10, 11].

The main objective of this study is to analyze the abrasive wear behavior of polymer gears through experimental testing and propose a method that can be used to determine the wear coefficient which represents the most crucial parameter for polymer gear design regarding the wear lifetime predictions. Although there are many well-established methods for the determination of the operational parameters of polymer and polymer composite gears [12, 13], such as gear temperature, wear behavior, and bending stress, as well as the methods for the gear performance prediction based on the specific material properties, and tribological testing of wear behavior [14-16], the wear coefficient assessment methodology presented in this research is unique in terms of simplicity. The wear prediction methodology, that will also be introduced, is based on Archard's wear formulation, which assumes that the wear depth is proportional to contact pressure and sliding distance. Providing that the surface wear of polymer gears is represented by a large set of geometrical, operational, and tribological parameters, all of these parameters will be included by the experimentally obtained wear coefficient. With the developed wear prediction model, the evaluation of the tooth surface wear can be described reasonably well, which reduces the need to perform time-consuming experimental tests. The novelty of this study is reflected in the methodology adopted for the wear coefficient assessment that is based on the employment of optical methods, i.e. the use of a digital microscope as well as the development of the wear prediction model, which is rather simplistic in terms of wear treatment. The contribution of the conducted study in the related scientific field is reflected in the fact that the developed numerical model can be implemented to reduce the need for time-consuming testing of gears and predict various tribological parameters with their influence on the behavior of polymer gears during their lifetime.

II. MATERIALS AND METHODS

Figure 1 shows the flowchart of the conducted study. As evidenced in Figure 1, the experimental study performed on polymer gears, is interconnected with the numerical model, as the proper value of the wear coefficient, which is necessary for the surface wear and accompanying parameters to be described, is imported into the model. Once the wear depth is calculated, the iterative numerical procedure updates the data on surface wear and calculates the new contact conditions for the next iteration.

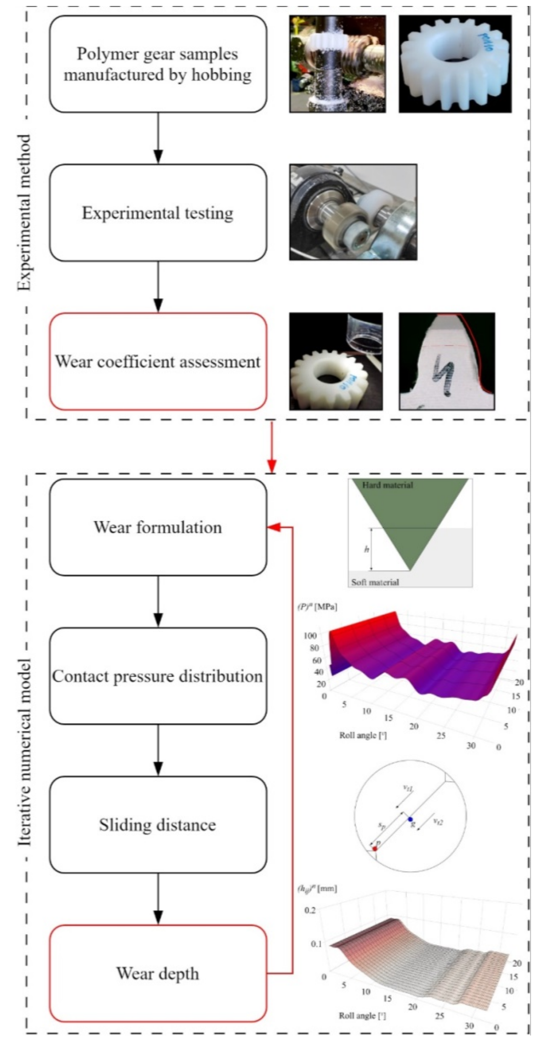

Fig. 1. Study flowchart.

A. Experimental Test Rig Configuration

To test polymer gears and obtain the necessary wear coefficient, a custom-made open-loop test rig was developed. Figure 2 depicts the polymer gear test rig configuration.

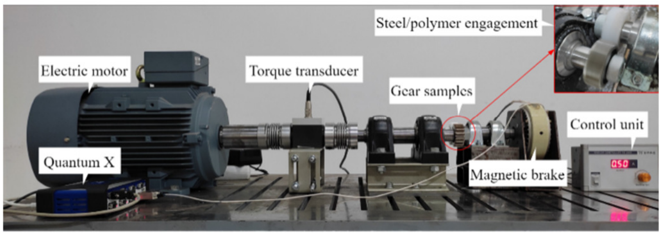

Fig. 2. Test rig configuration.

As observed in Figure 2, the polymer gear test rig is composed of an electric motor that is connected to the torque transducer, which is used for the measurement of torque and rotational speed. Torque transducer data acquisition is obtained with the Quantum X data acquisition system. The power, i.e. rotational motion, is supplied to the pinion, which is mounted at the end of the drive shaft through the system of couplings and bearings. Gear is mounted on the driven shaft, which is connected via bearing units to the magnetic powder brake used for precise load simulation, i.e. torque with a tension control unit. Open-loop configuration allows testing of various gear sizes, as the driven shaft can be precisely positioned in the horizontal direction to adjust the necessary center distance. The developed polymer gear test rig is designed for larger gear samples, where the geometry of tested samples is dictated according to the test rig's limitations and expected real-life applications [17].

B. Data on Polymer Gear Samples and Testing Conditions

To obtain the necessary wear coefficient, the scope of this research will cover classic steel/polymer engagements with a gear ratio of 1 and polymer gears made of Polyoxymethylene (POM) which are, due to the desired quality and smaller number of necessary samples, manufactured by hobbing with the basic geometrical parameters presented in Table I. Specific properties of the POM material are portrayed in Table II [18]. The aforementioned geometric parameters are defined according to the real-life applications of polymer gears with the same module, typically utilized in gear pumps and various conveyor systems. Although there is a wide scope of available polymer materials, POM material, as a high-performance thermoplastic, was chosen because of its beneficial sliding and thermal properties, as well as its ease of production, i.e. suitability for precision parts that require dimensional stability. Compared to other polymer materials, POM is attributed to high fatigue strength, low friction, and satisfactory chemical resistance. Experimental testing was conducted on ten POM gears with a load level of 4 Nm, which can be expected in real-life applications. Each of the ten tests was carried out at the rotational speed of 1000 rpm with a stopping criterion of 6 million cycles that was determined by performing preliminary tests. After the stopping criterion limit, tooth cross-section reduction affects the occurrence of plastic deformations that can lead to an unreliable assessment of the wear coefficient.

TABLE I. BASIC GEOMETRICAL PARAMETERS OF POLYMER GEARS

Property	Value
Module	3 mm
Number of teeth	17
Pressure angle	20°
Face width	20 mm
Profile shift factor	0
Pitch diameter	51 mm
Tip diameter	57 mm
Root diameter	44.4 mm
Base diameter	47.92 mm
Standard profile	Involute, ISO 53 A

TABLE II. SPECIFIC PROPERTIES OF POM MATERIAL

Property	Value	Test method
Density	1800 kg/m^3	ISO 1183
Tensile modulus	2000 MPa	ISO 527-2
Tensile strength	50 MPa	ISO 527-2
Linear expansion factor	$1.2 \cdot 10^{-4}$K^{-1}	ISO11359
Thermal conductivity	0.2 W/(K·m)	ISO 22007-4
Melting temperature	169 °C	DIN 53765

C. Wear Coefficient Assessment

When the testing is completed, all of the polymer gear samples are examined with the use of a digital microscope. The worn-out tooth profiles are measured with the 2D view at 22-fold magnification and compared to the initial tooth profile to determine the average linear wear W_m, as displayed in Figure 3. Implementing the specialized PortableCapture Plus 3.1 software, each worn-out tooth was measured five times at 250 different points along the tooth profile. As the polymer gear samples have 17 teeth, and experimental testing was conducted on 10 samples, a total of 215000 measurements were carried out to thoroughly establish the necessary wear coefficient. The established mean value of the wear coefficient, with the associated statistical parameters obtained with Minitab v20.4 software, are provided in Table III. As manifested in Table III, the mean value of the wear coefficient amounts to $5.6 \cdot 10^{-6}$ mm^3/(Nm), with a standard deviation of 0.3143 mm^3/(Nm), and a standard error mean value of 0.0994 mm^3/(Nm). The values of statistical parameters, indicate the negligible dispersion of the experimental data thereby confirming the relevance of the acquired wear coefficient.

The average linear wear W_m is defined as the longest perpendicular distance between the initial and worn-out tooth profile and for the tested gear samples it is located around the pitch diameter, as detected in Figure 3. The measured value of the average linear wear W_m is used to calculate the wear coefficient k_w, by employing the abrasive wear model proposed by the VDI 2736 guidelines for polymer gear design [19, 20], which is:

$$k_w = \frac{W_m b_w z l_{Fl}}{2\pi T_d N_L H_V} \quad (1)$$

where b_w is the common face width (mm), z is the number of teeth (-), l_{Fl} is the length of the profile line (mm), T_d is the nominal torque (Nm), N_L is the number of working cycles, i.e. stopping criterion, and H_V is the tooth degradation factor (-).

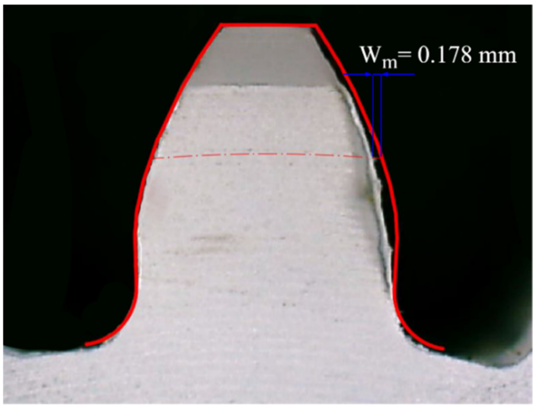

Fig. 3. Measurement of the worn-out tooth profile.

TABLE III. EVALUATED WEAR COEFFICIENT AND ASSOCIATED STATISTICAL PARAMETERS

Property	Value
Wear coefficient mean value	$5.6\cdot10^{-6}$ $mm^3/(Nm)$
Standard error mean value	0.0994 $mm^3/(Nm)$
Standard deviation	0.3143 $mm^3/(Nm)$

D. Modeling of Polymer Gear Wear

1) Wear Fformulation

The wear prediction methodology employs Archard's wear formulation with the assumption of unchanged hardnesses of contacting surfaces [21, 22]. For a specific point of a polymer gear tooth flank, Archard's wear equation can be defined as:

$$\frac{dh}{ds} = k_w P \quad (2)$$

where h is the wear depth for a specific point of polymer gear tooth flank (mm), s is the sliding distance (mm), and P is the local contact pressure (MPa).

As observed in (2), the wear formulation uses the experimentally obtained wear coefficient k_w, to fully describe the complexity of the engagement problem. If (2) is integrated over s, the wear depth of any point of the polymer gear tooth flank during one engagement cycle can be defined as:

$$h^{(n)} = h^{(n-1)} + k_w P^{(n-1)} s \quad (3)$$

where $h^{(n-1)}$ is the wear depth of a specific from the previous cycle (mm), $P^{(n-1)}$ is the local contact pressure at the specific point from the previous cycle (MPa), and n is the current cycle, i.e. iteration step for progressive wear formulation (-).

2) Contact Pressure Distribution

The most challenging task of the wear model development is the prediction of the contact pressure distribution. The methodology employed here determines the pressure of a specific point by modeling the contact surfaces with Winkler's foundation model, where the displacement of a specific contact point is a local function of pressure [23, 24]. The contact surfaces are represented as a set of elastic springs evenly distributed by a distance of Δx, as shown in Figure 4.

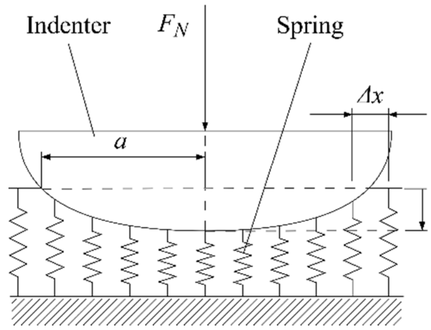

Fig. 4. Winkler's foundation model.

To determine the pressure of a specific contact point, the indentation d needs to be identified so that the normal applied load per unit length F_N satisfies the condition:

$$F_N = \Delta k_z A \quad (4)$$

where Δk_z is the stiffness of individual spring (N/mm) and A is the contact area (mm^2) defined with contact half-width a (mm).

According to Winkler's hypothesis, the contact pressure P at the contact point of the tooth flank can be expressed by:

$$P = C_W(d - f - h) \quad (5)$$

where C_W is the Winkler's modulus (Pa/mm) and f is the initial gap function (mm).

The determination of Winkler's modulus C_W is evaluated based on the correlation with the results of Hertzian solutions for typical non-conformal contacts regarding the maximum contact pressure or the size of contact area, or good agreement between both. In the present study, the maximum contact pressure with Winkler's surface model is determined based on the maximum Hertzian pressure, where Winkler's modulus amounts to $C_W = 2880$ MPa/mm.

3) Sliding Distance

The sliding distance calculation is also based on the Hertzian theory, where the surfaces at the current engagement position can be thought of as equivalent cylinders with variable diameters [25, 26], with the sliding distances of gear and pinion, s_p and s_g, defined with (6) and (7), respectively:

$$s_p = 2a(1 - v_{t2}/v_{t1}) \quad (6)$$

$$s_g = 2a(1 - v_{t1}/v_{t2}) \quad (7)$$

where v_{t1} is the tangential velocity of the specific contact point on pinion (m/s) and v_{t2} is the tangential velocity of the specific contact point on gear (m/s).

As the gear tooth contact operates under the combined motions of sliding and rolling, where theoretical sliding at the pitch diameter is zero due to pure rolling, the wear formulation defined with (3) also results in zero wear depth at the same zone [27, 28]. Considering that polymer gear deflection will in realistic cases result in wear even at the pitch diameter, the developed model calculates the sliding distances at the pitch zone by employing the values from adjacent contact points.

III. RESULTS AND DISCUSSION

Supposing that the solution of the previously described wear model depends on the surface parameters, i.e. changes that occur on the contact surface due to the wear mechanism, the developed model is based on the Boundary Element Method (BEM). The wear model is adjusted so that the prediction of polymer gear surface wear and contact pressure is computed at different rotational positions r. The number of these rotational positions, considering the gear geometry presented in Table I is 250, which corresponds to the rotational increment of 0.128°. The number of rotational positions r, namely the rotational increment, was chosen to fit the contact analysis problem, as the contact half-width a is much smaller than the other geometrical parameters requiring a very fine mesh used to describe a complete wear cycle from the point where tooth enters and exits the engagement [29, 30].

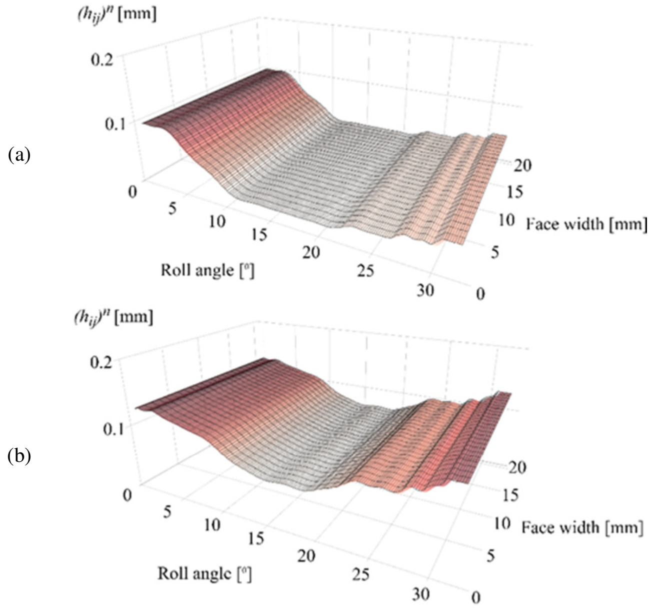

Fig. 5. Wear depth: (a) $1\cdot10^6$ cycles, (b) $2.5\cdot10^6$ cycles.

The developed model was employed to conduct several case studies of changes in wear depth and contact pressure distribution of the POM gear tooth flank at the load level of 4 Nm that corresponds to the previously established wear coefficient. Figure 5(a) exhibits the wear depth $(h_{ij})^n$ of POM gears after $1\cdot10^6$ cycles, where i and j denote the node index of a mesh grid in roll angle and face width directions, respectively. As disclosed in Figure 5(a), the most significant wear is observed for roll angles less than 4°, which corresponds to the tooth root area of the POM gear, with negligible wear at the pitch diameter zone (roll angle of 16.5°) and a slight increase of wear at the tooth tip area. The maximum wear depth at the tooth root area amounts to 0.097 mm. The wear depth for $2.5\cdot10^6$ cycles, provided in Figure 4(b), demonstrates the further increase in wear along the active profile. The wear intensity of the tooth root area decreases as the altered contact pattern shifts to the pitch diameter and tooth tip zones, increasing the wear intensity, as shown in Figure 5(b), with the maximum wear depth of 0.117 mm for the roll angles greater than 30°.According to the existing numerical models developed to describe the wear behavior of polymer gears, the highest wear depth after a certain number of working cycles is mainly located around the starting and ending engagement points [31, 32]. Although these models can predict the wear depth at the early stages of engagement reasonably well, they are mainly based on a theoretical approach suggesting that the wear at the pitch line is zero owing to kinematical contact with pure rolling, that is, zero sliding which results in unrealistic zero wear depth at the pitch line. Considering the real working conditions at which the teeth of polymer gears will most certainly deflect due to weaker and temperature-dependent material properties, the approach presented in this study takes into consideration this effect by calculating the sliding distance at the pitch line based on the values of sliding distances at adjacent points, which results in non-zero wear at the pitch line zone.

Figure 6(a) illustrates the initial (zero wear) contact pressure distribution with the maximum pressures located around the start and the end of the engagement (roll angles of 0° and 33°, respectively), and around the pitch line due to the single-tooth pair engagement period. The initial contact pressure distribution, as obvious from the presented Winkler's surface model, is fully correspondent to the Hertzian contact [23]. The contact pressure spikes at the start and the end of the engagement (roll angles of 0° and 33°, respectively) are not to be expected in real-life applications, since the tooth modifications such as tip relief and fillet rounding will result in slightly lower contact pressures, as simulated with other existing models [1, 10]. Although these models provide a more realistic analysis of contact pressures at the initial contact conditions at the start and the end of the engagement, they are mainly based on the Finite Element Method (FEM) analysis obtained by commercial software, which makes them computationally heavy and limited regarding the contact analysis of continuous wear cycles [28]. Contact pressure distribution after $1\cdot10^6$ cycles, as exhibited in Figure 6(b), reveals a general increase in contact pressures with the patterns that follow the corresponding wear distribution. The decrease of contact pressures for roll angles less than 2° is attributed to changes in wear intensity, i.e. the decrease of wear mechanism, while the maximum contact pressure of 70 MPa is located at the tooth tip (roll angle of 33°). Figure 6(c) presents the contact pressure distribution after $2.5\cdot10^6$ cycles, with a decrease of contact pressure for roll angles less than 5° due to a reduction of wear intensity. The increase of contact pressures, shown in Figure 6(c), is shifted to the rest of the active profile for roll angles greater than 7°, with the maximum value located at the tooth tip, which amounts to 115 MPa.

To validate the presented model, experimental testing was conducted on several polymer gear samples that were stopped after an arbitrary number of cycles. Figure 7(a) portrays the comparative view of the tooth profile after $2\cdot10^6$ cycles attained with a digital microscope and simulated profile with the maximum measured deviation of 6.3% at the tooth tip. Figure 7(b) depicts the comparative view of the tooth profile after $3.7\cdot10^6$ cycles with a maximum deviation of 8.2% between the measured and the simulated profile. The maximum deviation of 8.2% is located above the pitch line zone.

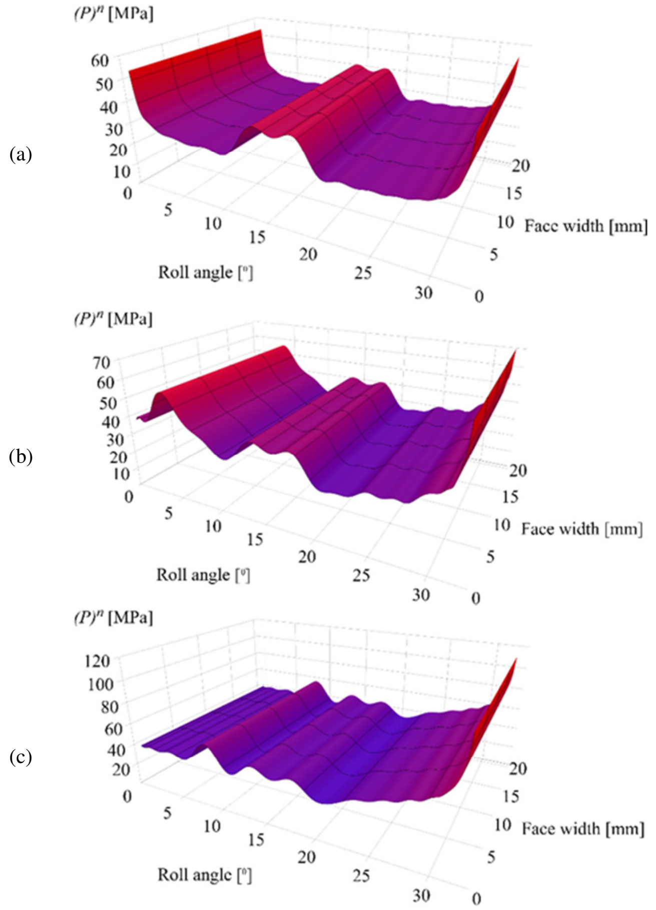

Fig. 6. Contact pressure distribution: (a) Initial distribution, (b) $1 \cdot 10^6$ cycles, (c) $2.5 \cdot 10^6$ cycles.

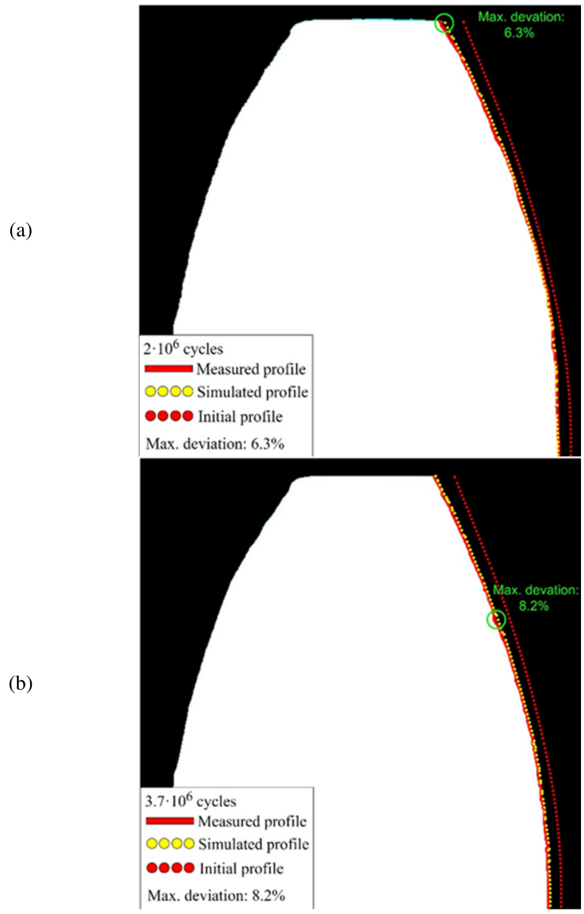

Fig. 7. Comparative view of measured and simulated tooth profiles with maximum deviation: (a) $2 \cdot 10^6$ cycles, (c) $3.7 \cdot 10^6$ cycles.

To fully compare the prediction errors of the wear prediction model stated in (3), where the wear depth h of the specific point is proportional to the contact pressure P and sliding distance s, the evaluation index of the prediction performance, namely the coefficient of determination R^2, is acquired through Minitab v20.4 software by comparing the simulation results with the measured values. The closer the value of R^2 is to 1, the closer the simulation results are to the real values. Accordingly, the R^2 of the presented prediction model amounts to 0.9314, which suggests that the fitting degree of the wear prediction model stated in (3) is high. Additionally, compared to the other existing numerical models [31, 32], the R^2 of the presented model is insensitive to the number of working cycles. Although these models can predict the wear depth for the smaller number of working cycles reasonably well (R^2>0.9), the previously mentioned theoretical approach followed in these models leads to a decrease in the coefficient of determination, as the wear simulation for the greater number of working cycles results in the increase of prediction error primarily in the pitch line zone [31, 32].

IV. CONCLUSION

This study analyzes the wear mechanism of POM gears in classic steel/polymer engagement and proposes a methodology to determine the necessary wear coefficient that can be utilized to predict the lifespan of polymer gears in real-life applications. Also, the same wear coefficient can be used as an input for the iterative numerical procedure for the prediction of wear depth. The main conclusions of the presented research are:

- The assessment of the wear coefficient presented within this study is unique in terms of simplicity, as it provides fast and reliable results that can be obtained with the employment of optical methods. The wear coefficient determination needs to correspond to the load conditions that to the greatest extent possible replicate the actual working conditions. The wear coefficient value of $k_w = 5.6 \cdot 10^{-6}$ mm^3/(Nm) with a standard deviation of 0.3143 mm^3/(Nm) can be deployed for lifetime predictions in real-life applications with similar gear geometry and material properties.
- Compared to the existing models that describe the wear behavior of polymer gears, the model introduced in this study results in realistic wear depth calculation, as the non-zero wear depth at the pitch line zone is expected due to the deflection of gear teeth. This problem is treated by taking

into consideration the sliding distances from the adjacent points at the pitch line zone. The conducted case studies for $1 \cdot 10^6$ and $2.5 \cdot 10^6$ cycles, with wear depths of 0.02 mm and 0.047 mm, respectively, demonstrate the benefits of this approach.

- The contact pressure distribution at the initial contact conditions (zero wear), which is fully correspondent with the Hertzian distribution, results in contact pressure spikes of 53 MPa at the start and the end of the engagement (roll angles of 0° and 33°, respectively) that are not likely to be expected in the actual working conditions, as the tooth modifications, such as tip relief and fillet rounding have a great impact on the contact pressures. Since the current version of the developed model considers only the theoretical involute profile, further development of the model should be directed toward the proper treatment of these modifications.
- The model validation shows good agreement between the measured and simulated tooth profiles with maximum deviations of 6.3% and 8.2% for the analyzed profiles after $2 \cdot 10^6$ and $3.7 \cdot 10^6$ cycles, respectively, suggesting that, despite being simple, the presented wear prediction model is sufficient for most engineering applications provided that the wear coefficient of the analyzed polymer material is addressed properly and the contact pressure distribution is predicted reasonably well.

REFERENCES

[1] D. Zorko, S. Kulovec, J. Duhovnik, and J. Tavčar, "Durability and design parameters of a Steel/PEEK gear pair," *Mechanism and Machine Theory*, vol. 140, pp. 825–846, 2019, https://doi.org/10.1016/j.mechmachtheory.2019.07.001.

[2] S. Matkovič, A. Pogačnik, and M. Kalin, "Wear-coefficient analyses for polymer-gear life-time predictions: A critical appraisal of methodologies," *Wear*, vol. 480–481, 2021, https//doi.org/10.1016/j.wear.2021.203944.

[3] K. A. M. Alharbi, "Wear and mechanical contact behavior of polymer gears," *Journal of Tribology*, vol. 141, no. 1, 2019, Art. no. 011101, https://doi.org/10.1115/1.4041020.

[4] D. G. Zisopol, A. I. Portoaca, I. Nae, and I. Ramadan, "A Statistical Approach of the Flexural Strength of PLA and ABS 3D Printed Parts," *Engineering, Technology & Applied Science Research*, vol. 12, no. 2, pp. 8248-8252, 2022, https://doi.org/10.48084/etasr.4739.

[5] D. G. Zisopol, I. Nae, A. I. Portoaca, and I. Ramadan, "A Theoretical and Experimental Research on the Influence of FDM Parameters on Tensile Strength and Hardness of Parts Made of Polylactic Acid," *Engineering, Technology & Applied Science Research*, vol. 11, no. 4, pp. 7458-7463, 2021, https://doi.org/10.48084/etasr.4311.

[6] S. M. Evans and P. S. Keogh, "Wear mechanisms in polyoxymethylene spur gears," *Wear*, vol. 428–429, pp. 356–365, 2019, https://doi.org/10.1016/j.wear.2019.03.027.

[7] A. Kumar Singh and Siddhartha, "Thermal and Wear Behavior of Glass Fiber-Filled Functionally Graded Material-Based Polyamide 66 Spur Gears Manufactured by a Novel Technique," *Journal of Tribology*, vol. 140, no. 2, 2018, https://doi.org/10.1115/1.4037335.

[8] J. Tavcar, G. Grkman, and J. Duhovnik, "Accelerated lifetime testing of reinforced polymer gears," *Journal of Advanced Mechanical Design, Systems and Manufacturing*, vol. 12, no. 1, 2018, https://doi.org/10.1299/jamdsm.2018jamdsm0006.

[9] P. K. Singh, Siddhartha, and A. K. Singh, "An investigation on the thermal and wear behavior of polymer based spur gears," *Tribology International*, vol. 118, pp. 264–272, 2018, https://doi.org/10.1016/j.triboint.2017.10.007.

[10] J. Tavčar, B. Cerne, J. Duhovnik, and D. Zorko, "A multicriteria function for polymer gear design optimization," *Journal of Computational Design and Engineering*, vol. 8, no. 2, pp. 581–599, 2021, https://doi.org/10.1093/jcde/qwaa097.

[11] A. Rohrmoser, C. Bode, B. Schleich, H. Hagenah, S. Wartzack, and M. Merklein, "Influence of metal gear tooth geometry on load and wear within metal-polymer gear pairs," *Applied Sciences*, vol. 12, no. 1, 2022, Art. no. 270, https://doi.org/10.3390/app12010270.

[12] S. H. Budapanahalli, S. B. Mallur, A. Y. Patil, and S. C. Dhaduti, "Experimental Investigation on Hybrid Aluminium Metal Matrix Composite Spur Gears," *Journal of The Institution of Engineers (India): Series D*, Jan. 2024, https://doi.org/10.1007/s40033-024-00646-3.

[13] S. C. Dhaduti, S. G. Sarganachari, A. Y. Patil, S. H. Budapanahalli, and R. Kumar, "Asymmetric/Symmetric Glass-Fibre-Filled Polyamide 66 Gears—A Systematic Fatigue Life Study," *Journal of Composites Science*, vol. 7, no. 9, Sep. 2023, Art. no. 345, https://doi.org/10.3390/jcs7090345.

[14] S. C. Dhaduti, S. G. Sarganachari, A. Y. Patil, and T. M. Yunus Khan, "Prediction of injection molding parameters for symmetric spur gear," *Journal of Molecular Modeling*, vol. 26, no. 11, 2020, Art. no. 302, https://doi.org/10.1007/s00894-020-04560-9.

[15] S. H. Budapanahalli, S. B. Mallur, A. Y. Patil, and R. Kumar, "Optimization study on wear behaviour of aluminium 7075 hybrid composite containing silicon carbide and aluminium oxide using Taguchi method," *Acta Periodica Technologica*, no. 54, pp. 129-136, 2023, https://doi.org/10.2298/APT2354129B.

[16] S. H. Budapanahalli et al., "A Tribological Study on the Effect of Reinforcing SiC and Al2O3 in Al7075: Applications for Spur Gears," *Metals*, vol. 12, no. 6, 2022, Art. no. 1028, https://doi.org/10.3390/met12061028.

[17] B. Zhong, R. Zhang, P. Wei, H. Liu, J. Li, and Z. Lu, "The Durability Performance of Polyketone Gears under Various Lubrication Conditions," *Journal of Tribology*, vol. 144, no. 9, 2022, Art. no. 091203, https://doi.org/10.1115/1.4054140.

[18] "MatWeb: Material Property Data," *MatWeb LLC*, 2022. https://www.matweb.com.

[19] S. Matkovič, A. Pogačnik, and M. Kalin, "Comparison between VDI 2736 wear calculation and experimentally obtained results," in *International Conference on Gears 2019*, 2019, pp. 1311–1322, https://doi.org/10.51202/9783181023556-1311.

[20] *VDI 2736 Part 2; Thermoplastic Gear Wheels—Cylindrical Gears—Calculation of the Load—Carrying Capacity*. Harzgerode, Germany: Verein Deutscher Ingenieure, 2016.

[21] Q. Li, F. Forsbach, M. Schuster, D. Pielsticker, and V. L. Popov, "Wear analysis of a heterogeneous annular cylinder," *Lubricants*, vol. 6, no. 1, 2018, Art. no. 28, https://doi.org/10.3390/lubricants6010028.

[22] A. Kahraman and H. Ding, "A methodology to predict surface wear of planetary gears under dynamic conditions," *Mechanics Based Design of Structures and Machines*, vol. 38, no. 4, pp. 493–515, 2010, https://doi.org/10.1080/15397734.2010.501312.

[23] N. Menga and M. Ciavarella, "A Winkler solution for the axisymmetric Hertzian contact problem with wear and finite element method comparison,"*Journal of Strain Analysis for Engineering Design*, vol. 50, no. 3, pp. 156–162, 2015, https://doi.org/10.1177/0309324714567489.

[24] S. Garcin, S. Baydoun, P. Arnaud, and S. Fouvry, "Fretting wear modeling of 3D and 2D Hertzian contacts with a third-body layer using a Winkler elastic foundation model," *Tribology International*, vol. 170, Jun. 2022, Art. no. 107493, https://doi.org/10.1016/j.triboint.2022.107493.

[25] Z. Liu, X. Xiao, W. Zhou, Z. Wang, H. Zhang, and J. Zhou, "Wear Analysis of Hot Extrusion Punch for Large Fan Shaft Based on Archard Wear Theory," in *Proceedings of the 14th International Conference on the Technology of Plasticity - Current Trends in the Technology of Plasticity*, 2024, pp. 371–380, https://doi.org/10.1007/978-3-031-41023-9_38.

[26] F. Di Puccio and L. Mattei, "Further Validation of a Simple Mathematical Description of Wear and Contact Pressure Evolution in

Sliding Contacts," *Lubricants*, vol. 11, no. 5, 2023, Art. no. 230, https://doi.org/10.3390/lubricants11050230.

[27] M. B. Sánchez, M. Pleguezuelos, and J. I. Pedrero, "Influence of profile modification on the transmission error of spur gears under surface wear," *Mechanism and Machine Theory*, vol. 191, Jan. 2024, Art. no. 105473, https://doi.org/10.1016/j.mechmachtheory.2023.105473.

[28] D. Zorko, J. Štiglic, B. Černe, and N. Vukašinović, "The effect of center distance error on the service life of polymer gears," *Polymer Testing*, vol. 123, Jun. 2023, Art. no. 108033, https://doi.org/10.1016/j.polymertesting.2023.108033.

[29] A. Dzierwa and P. Pawlus, "Wear of a rough disc in dry sliding contact with a smooth ball: experiment and modeling," *Archives of Civil and Mechanical Engineering*, vol. 21, no. 2, 2021, Art. no. 85, https://doi.org/10.1007/s43452-021-00240-4.

[30] A. Winkler, M. Bartz, and S. Wartzack, "Numerical Wear Modeling in the Mixed and Boundary Lubrication Regime," *Lubricants*, vol. 10, no. 12, 2022, Art. no. 334, https://doi.org/10.3390/lubricants10120334.

[31] A. Ignatijev, M. Borovinšek, S. Glodež, "A Computational Model for Analysing the Dry Rolling/Sliding Wear Behaviour of Polymer Gears Made of POM," *Polymers*, vol. 16, no. 8, 2024, Art. no. 1073, https://doi.org/10.3390/polym16081073.

[32] M. S. Tunalioglu and B. V. Agca, "Wear and Service Life of 3-D Printed Polymeric Gears," *Polymers*, vol. 14, no. 10, 2022, Art. no. 2064, https://doi.org/10.3390/polym14102064.